Proceedings of the 2004 IEEE
International Conference on Robotics & Automation
New Orleans, LA • April 2004

Constructing Radio Signal Strength Maps with Multiple Robots

Mong-ying A. Hsieh, Vijay Kumar and Camillo J. Taylor
GRASP Laboratory
University of Pennsylvania
Email: {mya, kumar, cjtaylor}@grasp.cis.upenn.edu

Abstract— **Communication is essential for coordination in most cooperative control and sensing paradigms. In this paper, we investigate the construction of a map of radio signal strength that can be used to plan multirobot tasks and also serve as useful perceptual information. We show how nominal models of an urban environment, such as those obtained by aerial surveillance, can be used to generate strategies for exploration and present preliminary experimental results with our multi-robot testbed.**

I. INTRODUCTION

There is a growing community of researchers in multi-agent robotics and sensor networks whose goal is to develop networks of sensors and robots that can perceive their environment and respond to it, anticipating information needs of the network users, repositioning and self-organizing themselves to best acquire and deliver the information. Communication is fundamental to most multi-agent coordinated tasks, such as, cooperative manipulation [1], multi-robot motion planning [2], collaborative mapping and exploration [3], and formation control [4]. Communication links are used to control the motion of the agents and for each agent to infer its location with respect to those of its neighbors and other landmarks. On the other hand, agents may also need to control their position and orientation relative to other agents to sustain communication links. While there is significant literature on multirobot control, sensing [5], planning [2], and localization [6], most of these papers focus on control and perception and assume that robots can freely communicate with each other.

Some recent papers have considered the effects of communication constraints. Reference [7] considers distributed multi-robot sensing and data collection where the individual robot's communication range is assumed to be static. Decentralized controllers for concurrently moving toward goal destinations while maintaining communication constraints are discussed in [8]. The discrete motion planning problem of moving while maintaining visibility constraints is discussed in [9].

It is difficult, in general, to predict radio connectivity a priori since it depends upon a variety of factors including transmission power, terrain characteristics, and interference from other sources [10]. This suggests if we can learn the communication characteristics of the environment online, we can generate a radio connectivity map that can be used in the planning and deployment of future tasks.

In this paper, we consider the problem of acquiring information to obtain such radio signal strength maps in an urban terrain. We formulate the problem as an exploration of an environment with known geometry, but one in which the radio transmission characteristics are unknown. We assume that overhead surveillance pictures, such as the one shown in Figure 2(a), can be used to automatically construct roadmaps for motion planning, and we formulate the radio connectivity map exploration problem as a graph exploration problem. We describe algorithms that allow small teams of robots to explore two-dimensional workspaces with obstacles to obtain a radio connectivity map. The salient feature of our work is that we reduce the exploration problem to a multirobot graph exploration problem, which we solve for teams of two and three robots.

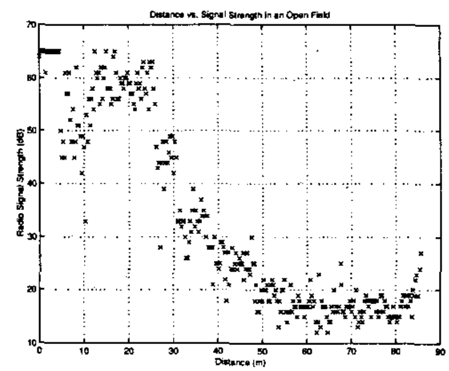

Fig. 1. Signal to noise ratio measurements of the radio signal strength as a function of transmission distance in an open field. Transmitters and antennas were positioned 18.5 inches above the ground and the signal strength (y-axis) is normalized to a scale of 0 - 65 dB.

This paper is organized as follows. In Section 2, we describe the terminology and notation used to model the problem. The methodology is described in Section 3 for the two robot and three robot problems. Section 4 and 5 summarizes the results for both the two and three robot cases and provide some discussion on the computational complexity of the proposed algorithms. Section 6 discusses some ongoing research in exploration and ideas for future work.

II. MODELING

For any given environment, denote the configuration space as $\mathcal{C}$ and the obstacle free portion of $\mathcal{C}$ as $\mathcal{C}_f$, also referred as the free space. Given any two positions $q_i, q_j \in \mathcal{C}_f$, the *radio*

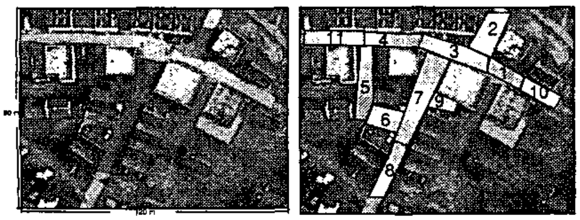

Fig. 2. (a) A typical surveillance picture from our fixed wing UAV taken at an altitude of 150 m. (b) Example of a cell decomposition of the free configuration space for the site shown in Figure 2(a).

connectivity map is a function $\varphi : (q_i, q_j) \rightarrow \mathbb{R}$ that returns the radio signal strength between the two positions given by q_i and q_j. To obtain a connectivity map for all pairs of positions in $\mathcal{C}_f$ is extremely difficult, instead, we propose to construct a map for pairs of locations in the set $Q = \{q_1, \ldots, q_{n_1}\}$ such that Q is a subset of $\mathcal{C}_f$.

We assume that a convex cell decomposition can be performed on any given $\mathcal{C}_f$ such that each location in the set Q is located within a cell. Since each cell is convex, it is possible to predict the signal strength between any two points given the line-of-sight property associated with points in a convex set and prior knowledge of the variation of radio signal transmission characteristics with distance. This does not necessarily mean the signal strenth will be the same for other pairs of positions in those two cells. However, we can effectively use the information about signal strength between a given pair of points and the knowledge of the transmission characterisitics within the cell to deploy a multirobot team that can communicate via a multi-hop network between any pair of points. Thus, we will assume the decomposition is given instead of solving the problem of determining the appropriate cell decomposition.

We further assume a connected roadmap which can be constructed from the given cell decomposition of $\mathcal{C}_f$ and computing the set of feasible paths between neighboring cells. Figure 2(b) is an example of a cell decomposition of $\mathcal{C}_f$ for the site shown in Figure 2(a). The undirected graph $G_1 = (V_1, E_1)$ is a representation of the roadmap where each cell is associated with a node in V_1 and every edge in the set E_1 represents a feasible path between neighboring cells. Given,

$$V_1 = \{v_1^1, \ldots, v_1^{n_1}\} \quad \text{and} \quad E_1 = \{e_1^1, \ldots, e_1^{m_1}\},$$

the total number of nodes and edges in G_1, are denoted as n_1 and m_1 respectively. Thus, G_1 is always connected and we will denote A_1 as the adjacency matrix for G_1 such that

$$A_1 = [a_{ij}] = \begin{cases} 1 & \text{if path exists between } v_1^i \text{ and } v_1^j \\ 0 & \text{otherwise} \end{cases}$$

We will call G_1 the *roadmap graph*.

Next, we define the *radiomap graph*, $R = (V_1, L_1)$, where L_1 is the set of links between pairs of nodes we would like to gather signal strength information for. The edge set L_1 is selected a priori based on the task objectives, the physical environment and prior knowledge of radio signal transmission characteristics and may include all possible edges in G_1. In other words, R encodes the information that must be obtained. We will denote A_R as the adjacency matrix for R such that

$$A_R = [a_{R_{ij}}] = \begin{cases} 1 & \text{if signal strength between } v_1^i \\ & \text{and } v_1^j \text{ is to be measured} \\ 0 & \text{otherwise} \end{cases}$$

The objective is to develop an optimal plan to measure the signal strength of every edge in L_1 given G_1. Thus, given the roadmap and radiomap graphs, G_1 and R, we define a third graph, which we will call the *multirobot exploration graph* and denote it as $G_k = (V_k, E_k)$ where k denotes the number of robots. We construct the multirobot exploration graph such that obtaining an optimal plan to measure the edges in L_1 is equivalent to solving for the shortest path on the graph G_k. We outline our methodology in the following section.

III. Methodology

Given the roadmap, $G_1 = (V_1, E_1)$, and k robots we define a *configuration* on the graph G_1 as an assignment of the k robots to k nodes of the graph. Figure 3(b) shows some possible configurations of three robots on the roadmap graph G_1, shown in Figure 3(a). Here solid vertices denote the locations of the robots. Since the graph G_1 is connected, a path always exists for k robots to move from one configuration to another. For certain configurations of k robots on G_1, the complete graph generated by taking the locations of the robots as vertices, contains some of the edges in L_1. Figure 4(b) shows some three robot configurations on G_1 that can measure edges in L_1, the edge set of the radiomap graph shown in Figure 4(a). Therefore, an optimal plan to measure all edges in the set L_1 can be viewed as a sequence of robot configurations such that every edge in L_1 is measured by at least one of these configurations.

In general, given the roadmap and radiomap graphs $G_1 = (V_1, E_1)$ and $R = (V_1, L_1)$ and k robots, the multirobot exploration graph, $G_k = (V_k, E_k)$, is constructed such that every node in V_k denotes a k-robot configuration on G_1 that measures a subset of L_1. An edge, $e_k^{ij} \in E_k$, exists between any two nodes $v_k^i, v_k^j \in V_k$ if the configuration associated with v_k^i is reachable from the configuration associated with v_k^j. Since G_1 is always connected, k robots can always move from one configuration to another, therefore, G_k is always a complete graph. To obtain an optimal plan, every edge in E_k is assigned a minimum cost that represents the total number of moves required to move the robots from one configuration to another.

For the configuration given by the nodes $\{2, 3, 4\}$ as shown in Figure 3(b), the cost to move to the configuration given by nodes $\{1, 2, 3\}$ is 2. The optimal plan would then be a sequence of configurations, such that moving through all configurations in the sequence results in covering all edges in L_1 while minimizing the number of total moves. In other words, finding an optimal plan is equivalent to solving for a minimum cost path on G_k that covers all the edges of L_1.

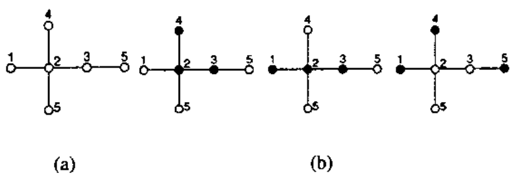

Fig. 3. (a) Roadmap graph, G_1. The solid edges denote feasible paths between neighboring cells associated with each node. (b) Three different configurations three robots can take on the graph G_1. The solid vertices denote the locations of the robots.

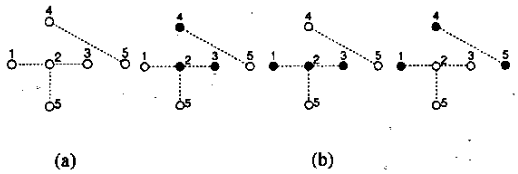

Fig. 4. (a) Radiomap graph, R_1, for G_1 shown in Figure 3(a). The dashed edges denote links for which signal strength information must be obtained. (b) Three sample configurations of three robots on G_1 that can measure at least one of the edges in R_1. The solid vertices denote the location of each robot.

We outline methods to construct G_k, for the two robot and three robot cases and solve for the respective optimal plans in the following sections.

A. Two Robot Problem

Given the roadmap and radiomap graphs $G_1 = (V_1, E_1)$ and $R = (V_1, L_1)$ and two robots, the maximum number of links that can be measured for any configuration is one. For the two robot case, the radio exploration graph $G_2 = (V_2, E_2)$ can be constructed such that each node in G_2 corresponds to one edge in the set L_1. For example, given the roadmap and radiomap graphs shown in Figure 5, Figure 6(a) shows the mapping of every edge in L_1 to a node in G_2. By computing the cost to move between every pair of nodes in G_2, we obtain the weight of every edge in E_2 as shown in 6(b). The minimum cost to move from the configuration $\{2, 6\}$ to $\{1, 5\}$, denoted by nodes $4'$ and $1'$ respectively in Figure 6(b), is equal to 2.

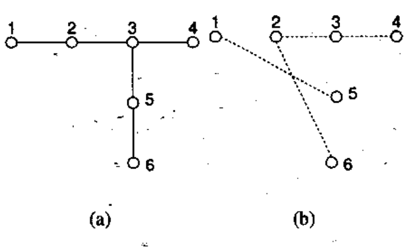

Fig. 5. (a) Roadmap graph, G_1. The solid edges denote feasible paths between neighboring cells associated with each node. (b) Radiomap graph, R. The dashed edges denote the links for which signal strength information must be gathered.

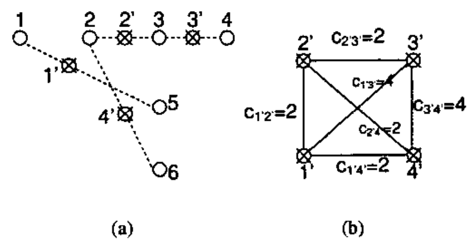

Fig. 6. (a) Graph R superimposed with G_2 nodes, denoted by $\otimes$. (b) The radio exploration graph, G_2, for the roadmap and radiomap graphs shown in Figure 5.

Thus, the edge $e_2^{4'1'}$ has a weight of 2. From this example, the optimal plan for a start configuration given by node $1'$ is the path $\{1', 4', 2', 3'\}$ with a total cost of 6 moves. For the two robot case, an optimal plan requires the traversal of every node on G_2 at most once. This is equivalent to solving a traveling salesman problem on the graph G_2.

Algorithm 1 describes the method used to obtain the optimal plan for the 2-robot case. To determine the weight of every edge in E_2, we compute the shortest path between every pair of nodes in G_1. The adjacency and cost matrices for G_2 are obtained by considering the set of allowable moves given by G_1 and the set of edges given by R. Once we have the adjacency and cost matrices for G_2, the optimal plan is obtained by solving an open path traveling salesman problem on G_2. Although the Traveling Salesman Problem is known to be NP-hard, there are known approximation algorithms that solves for the minimum cost path in polynomial time [11]. For small graphs the problem can be solved using branch and bound techniques [12].

B. Three Robot Problem

Given the roadmap and radiomap graphs, G_1 and R, the set of nodes in V_3 is obtained by considering all 3-robot configurations on the graph G_1 that contain at least one edge in L_1. For the roadmap and radiomap graphs given in Figure 5, Figure 7(a) shows some configurations that contain some edges in L_1. The configuration given by nodes $\{1, 5, 6\}$ would correspond to node $1'$ on G_3. Figure 7(b) is a subgraph of G_3 with the nodes associated with the configurations shown in Figure 7(a) as its vertices. The algorithm to obtain the vertex set V_3 is outlined in Algorithm 2.

Similar to the two robot case, shortest path computation between every node in G_1 is required to determine the weight of every edge in E_3. The algorithm used compute the cost and adjacency matrices for G_3 is outlined in Algorithm 3. Unlike the two robot case, every edge in the set L_1 may potentially be associated with more than one node in V_3. Thus, the optimal plan for the three robot case would result in a path that contains a subset of the nodes in V_3. For this example, an optimal plan starting at the configuration given by node $1'$ is the path $\{1', 2', 4'\}$ with a total cost of 4. Note the path does not contain node $3'$. Given a starting node on G_3, a greedy algorithm is

Algorithm 1 Computation of the optimal plan for 2-robots

Construction of the vertex set V_2
Given G_1, A_1 and R, A_R
$V_2 = 0$
for each node $v_1^1, \ldots, v_1^{n_1}$ **do**
  for each node $v_1^1, \ldots, v_1^{n_1}$ **do**
    if $A_R(i,j) = 1$ **then**
      $V_2 = V_2 \bigcup v_2^z$, where v_2^z denotes the vertex associated with v_1^i and v_1^j
    end if
  end for
end for
Computing the cost, C_2, and adjacency, A_2, matrices for G_2
for each node $(v_2^1 \ldots v_2^{n_2})$ **do**
  for each node $(v_2^1 \ldots v_2^{n_2})$ **do**
    if $v_2^i \neq v_2^j$ **then**
      determine number of moves required to move from v_2^i to v_2^j using A_1
      $A_2(i,j) = 1$
      $C_2(i,j) =$ number of moves
    end if
  end for
end for
Compute minimum cost open path on G_2 such that each node in V_2 is traversed only once

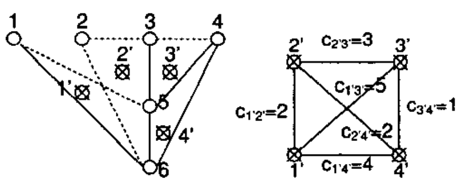

(a) (b)

Fig. 7. (a) Graph R overlayed with some G_3 nodes, denoted by $\otimes$. Node $3'$ refers to the configuration given by nodes $\{3,4,5\}$ while node $4'$ refers to the configuration given by nodes $\{3,4,6\}$. (b) Subgraph of the radio exploration graph, G_3, for the roadmap and radiomap graphs shown in Figure 5.

used to compute a path on G_3 such that traversal of each node on the path increases the number of measured edges in L_1. Thus, at any configuration, the next configuration is chosen as the one that increases the number of edges measured in L_1 and requires the least amount of moves to reach.

IV. Results

We present our two and three robot simulation results for the Military Operations on Urban Terrain (MOUT) training site located in Ft. Benning, Georgia for which radio signal strength data is important for operations such as surveillance and hostage rescue. Figure 2(a) is an aerial view of the MOUT site. More information on the experiments conducted at the

Algorithm 2 Construction of the vertex set of $G_3 = (V_3, E_3)$

Given G_1, A_1 and R, A_R
$V_3 = 0$
for each node $(v_1^1 \ldots v_1^{n_1})$ **do**
  for each node $(v_1^1 \ldots v_1^{n_1})$ **do**
    for each node $(v_1^1 \ldots v_1^{m_1})$ **do**
      if $v_1^i \neq v_1^j \neq v_1^k$ **then**
        if $(l_{ij}$, l_{jk} or $l_{ik} \in L_1)$ **then**
          $V_3 = V_3 \bigcup v_3^z$ where v_3^z denotes the vertex associated with v_1^i, v_1^j, v_1^k
        end if
      end if
    end for
  end for
end for

Algorithm 3 Computation of the adjacency and cost matrices, A_3 and C_3, for $G_3 = (V_3, E_3)$

Initialize A_3, C_3
for each node $(v_3^1, \ldots v_3^{n_3})$ **do**
  for each node $(v_3^1, \ldots v_3^{n_3})$ **do**
    if $v_3^i \neq v_3^j$ **then**
      Calculate minimum number of moves from v_3^i to v_3^j
      $A_3(i,j) = 1$
      $C_3(i,j) =$minimum number of moves
    end if
  end for
end for

MOUT site can be found in [13] and [14]. We assume a cell decomposition of the free space as shown in Figure 2(b). The roadmap and radiomap graphs are shown in Figure 8. Using the procedure outlined in the previous sections, we construct the graphs G_2 and G_3 and solve for their optimal plans. To improve on the computation time of our algorithm we only considered edges in E_2 with weights less than or equal to two moves and edges in E_3 with weights less than or equal to six moves.

A. Two Robot Problem

Using the methodology outlined in the previous section and restricting the edge set of E_2 to edges with cost no more than two moves, we compute a total of 23 nodes and 75 edges for the multirobot exploration graph G_2. The minimum cost open path starting with one robot at node 5 and one at node 6 as shown in Figure 8(a) requires a total of 28 moves to cover every last edge shown in Figure 8(b). Figure 10 shows the step by step execution of the plan.

B. Three Robot Problem

For the three robot problem, we compute a total of 139 nodes and 6045 edges for the multirobot exploration graph G_3 by considering edges with cost no more than six moves . The minimum cost path starting with robots at nodes 6, 7 and 9 as shown in Figure 8(a) traverses a total of 13 nodes in G_3

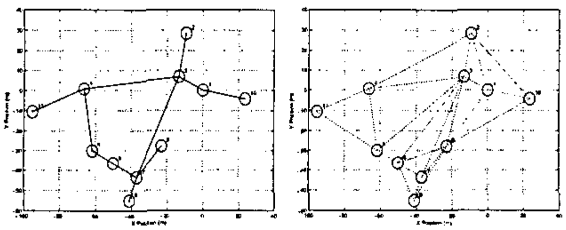

(a) (b)

Fig. 8. (a) Roadmap graph for the site shown in Figure 2(a). (b) Radiomap graph for the site shown in Figure 2(a).

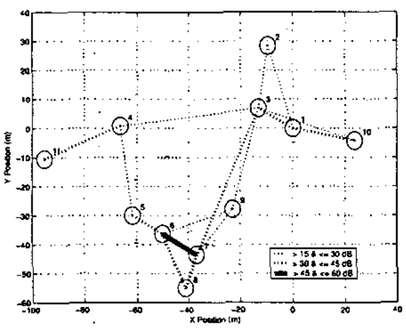

Fig. 9. Radio frequency map obtained by manually placing robots at each location associated with each node in G_1. Radio signal strength is normalized to a scale of 0 - 65 dB.

with a minimum cost of 31 moves. Figure 11 shows the step by step execution of the optimal plan.

Figure 9 shows a radio connectivity map for the MOUT site where the radio signal strength between any two locations are denoted by the different edges.

V. Discussion

Without considering the cost of computing a solution for the traveling salesman problem, the adjacency and cost matrices for G_2 given G_1 and R can be obtained in $O(n_2^3)$, where n_2 denotes the number of nodes in G_2. This is due to the need to compute shortest paths for all pairs of nodes in G_1. However, depending on the topology of G_1 and R, we could decrease the computation time by considering edges with weights no more than x number of moves. Similarly, for the three robot case, without considering the computation of the shortest path on G_3, the proposed methodology requires a run time of $O(n_3^3)$ where n_3 is the total number of nodes in G_3. It is worth noting that depending on the topology of R, it is possible to further reduce both the number of nodes and the number of edges in G_3 by enforcing stricter selection criterion when generating the vertex set outlined in Algorithm 2 and considering edges weighing no more than y number of moves in Algorithm 3. For example, if we only consider the set of nodes in G_1 such that every edge in the complete graph induced by the 3 robots is contained in L_1, then the number of nodes for G_3 can be reduced to a total of 15.

The difficulty in obtaining an optimal plan under the proposed methodology is the need to compute a minimum cost path on G_k such that every node on the path leads to measurement of every edge in L_1. Such minimum cost path computations are known to be extremely inefficient since the complexity is exponential in the number of nodes. For small graphs, the problem is solvable using branch and bound techniques. In general, the computational cost for finding a path on any G_k can be expensive and thus heuristic approaches need to be pursued.

VI. Future Work

In this work, we have addressed the case where the locations whose connectivity we wish to explore are given a priori. We hope to be able to address the problem of automatically selecting locations to be explored either by using overhead images which provide partial maps, or in the context of an online exploration process. Here we envision that we may want to consider the problem of selecting promising sites for communication relays. If we were able to identify and explore these locations efficiently we may choose to forgo the more laborious task of discovering the complete radio map of the site in favor of finding a set of locations that form an effective communication "skeleton" which allows us to span the site with communication links.

Similarly we can imagine focusing our exploration strategies to discover communication pathways that support the transmission of information from a particular area of interest back to the base station. This might be appropriate in situations where the users are interested in monitoring a particular area of the site.

Furthermore, it is often the case that the exploration of the radio map of the scene is being carried out concurrently with other activities such as environmental monitoring or situational awareness. Thus, another area which we plan to address is pursuing the radio mapping with other objectives and which must be effectively balanced against the other mission goals.

The ability to measure the strength of radio links between members of our mobile robot teams opens up many avenues for future work. We can imagine using the measurements gleaned from the robots to construct models for the transmission characteristics of the site. Since the rate of signal strength falloff with distance depends upon the composition of the materials in the environment and the geometry of the scene, it may be difficult to predict this relationship accurately before exploration. However, once the robots start their exploration we may be able to model this relationship effectively from measurements. These models could then be used to predict radio connectivity between locations that have not been visited.

Additional details and figures are available at http://www.seas.upenn.edu/ mya/publications/icra04-tech.pdf.

Acknowledgment

The authors would like to thank Luiz Chaimowicz, Dan Gomez-Ibanez, Anthony Cowley, Ben Grocholsky, Selcuk

Bayraktar, and Jim Keller (University of Pennsylvania) for help in collecting the data in the Figures 1, 2(a), 2(b), and 9, and Jason Redi and Keith Manning (BBN) for discussions on radio signal transmission characteristics. We greatfully acknowledge the support of DARPA grant MARS NBCH1020012, ARO MURI Grant DAAD19-02-01-0383, and NSF grant CCR02-05336.

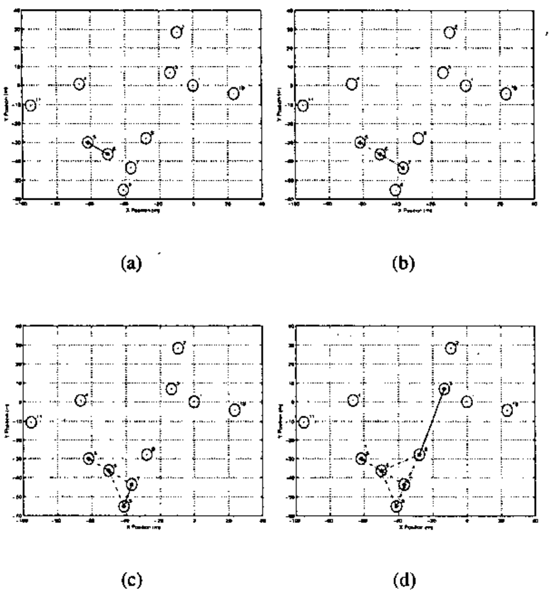

Fig. 10. Solid line denotes the current link being measured while a dotted line denotes a link that has been measured. (a) Starting configuration. (b) Second link to be measured. (c) Fourth link. (d) Eigth link.

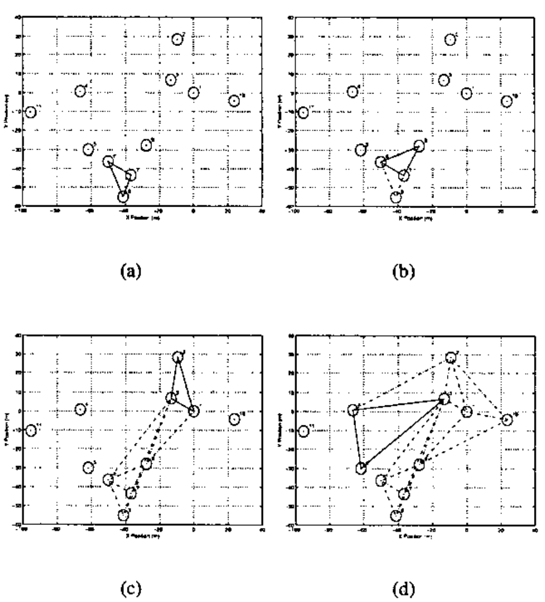

Fig. 11. Solid line denotes the current link being measured while a dotted line denotes a link that has been measured. (a) Starting configuration. (b) Second configuration. (c) Seventh configuration. (d) Eleventh configuration.

REFERENCES

[1] W. Kang, N. Xi and A. Sparks, "Formation control of autonomous agents in 3D workspace, " *Proc. IEEE Int. Conf. Robot. and Automat.*, San Francisco, CA, April 2000, pp. 1755-1760.

[2] Y. Guo and L. E. Parker, "A distributed and optimal motion planning approach for multiple mobile robots," *Proc. IEEE Int. Conf. Robot. and Automat.*, Washington, DC, 2002, pp. 2612-2619.

[3] W. Burgard, M. Moors, D. Fox, R. Simmons, and S. Thrun, "Collaborative Multi-Robot Exploration," *Proc. IEEE Int. Conf. Robot. and Automat.*, San Francisco, CA, April 2000, pp. 476-481.

[4] R. Fierro, P. Song, A. Das, and V. Kumar, "Cooperative Control of Robot Formations," *Cooperative Control and Optimization: Series on Applied Optimization*, Eds. R. Murphey and P. Paradalos, Kluwer Academic Press, 2002: 79-93.

[5] J. Cortes, S. Martinez, T. Karatas, and F. Bullo, "Coverage control for mobile sensing networks," *Proc. IEEE Int. Conf. Robot. and Automat.*, Washington, DC, May 2002, pp. 1327-1332.

[6] S. I. Roumeliotis and G. A. Bekey, "Distributed multi-robot localization," *IEEE Trans. on Robot. and Automation*, vol. 18, pp. 781-795, October, 2002.Thus, instead of solving the problem of determining the appropriate cell decomposition, we will assume the decomposition is given.

[7] A. F. T. Winfield, "Distributed sensing and Data Collection Via Broken Ad Hoc Wireless Connected Network of Mobile Robots," *Distributed Autonomous Robotic Systems 4*, Eds. L. E. Parker, G. Bekey and J. Barhen, Springer-Verlag, pp. 273-282, 2000.

[8] G. A. S. Pereira, A. K. Das, V. Kumar, and M. F. M. Campos, "Decentralized Motion Planning for Multiple Robots subject to sensing and communication constraints," *Proceedings of the Second Multi-Robot Systems Workshop*, Washington, DC, USA, March 2003, pp. 267-278.

[9] H. H. Gonzalez-Banos, L. Guibas, J.-C. Latombe, S.M. LaValle, D. Lin, R. Motwani, and C. Tomasi, "Motion Planning with Visibility Constraints: Building Autonomous Observers," *Proceedings of the Eighth International Symposium of Robotics Research*, Hayama, Japan, Oct. 1997.

[10] A. Neskovic, N. Neskovic, and G. Paunovic, "Modern Approaches in Modeling of Mobile Radio Systems Propagation Environment," *IEEE Communications Surveys*, Third Quarter 2000.

[11] *Traveling Salesman Homepage* `http://www.math.princeton.edu/tsp/`

[12] E. Horowitz, S. Sahni and S. Rajasekaran, *Computer Algorithms*. New York, New York, USA: Computer Science Press, 1998.Thus, instead of solving the problem of determining the appropriate cell decomposition, we will assume the decomposition is given.

[13] L. Chaimowicz, Ben Grocholsky, J. F. Keller, V. Kumar and C. J. Taylor, "Experiments in Multirobot Air-Ground Coordination," *Submitted to the International Conference on Robotics and Automation.*

[14] F. Zhang, B. Grocholsky and V. Kumar, "On Localization of Distributed Robot-Sensor Networks," *Submitted to the International Converence on Robotics and Automation.*

[15] A. Das, J. Spletzer, V. Kumar and C. J. Taylor, "Ad Hoc Networks for Localization and Control," *IEEE Conference on Decision and Control*, Las Vegas, 2002.

[16] I. M. Rekleitis, G. Dudek and E. E. Milios, "Graph-Based Exploration using Multiple Robots," *5th International Symposium on Distributed Autonomous Robotic Systems (DARS) 2000*, Knoxville, Tennessee, USA, October 4-6, 2000.

[17] P. Švestka and M. H. Overmars, "Probabilistic Path Planning," *Robot Motion Planning and Control*, Ed. J. P. Laumond, `http://www.laas.fr/~jpl/book.html`

[18] A. Howard, S. Siddiqi and G. Sukhatme, "An Experimental Study of Localization Using Wireless Ethernet," Proc. of the 4th Int. Conf. on Field and Service Robotics (FSR) 2003, Lake Yamanaka, Japan, July 2003.